Science Advances
AAAS

advances.sciencemag.org/cgi/content/full/6/12/eaaz3367/DC1

Supplementary Materials for

TRPC1 participates in the HSV-1 infection process by facilitating viral entry

DongXu He, AiQin Mao, YouRan Li, SiuCheung Tam, YongTang Zheng, XiaoQiang Yao, Lutz Birnbaumer, Indu S. Ambudkar*, Xin Ma*

*Corresponding author. Email: maxin@jiangnan.edu.cn (X.M.); indu.ambudkar@nih.gov (I.S.A.)

Published 18 March 2020, *Sci. Adv.* **6**, eaaz3367 (2020)
DOI: 10.1126/sciadv.aaz3367

This PDF file includes:

Fig. S1. Features of SOCE during HSV-1 infection.
Fig. S2. TRPC1 modulates HSV-1 infection.
Fig. S3. Dynamic changes of SOCE-related molecules during HSV-1 infection.
Fig. S4. Determination of gD-TRPC1 interaction.
Fig. S5. Original images of Western blots.

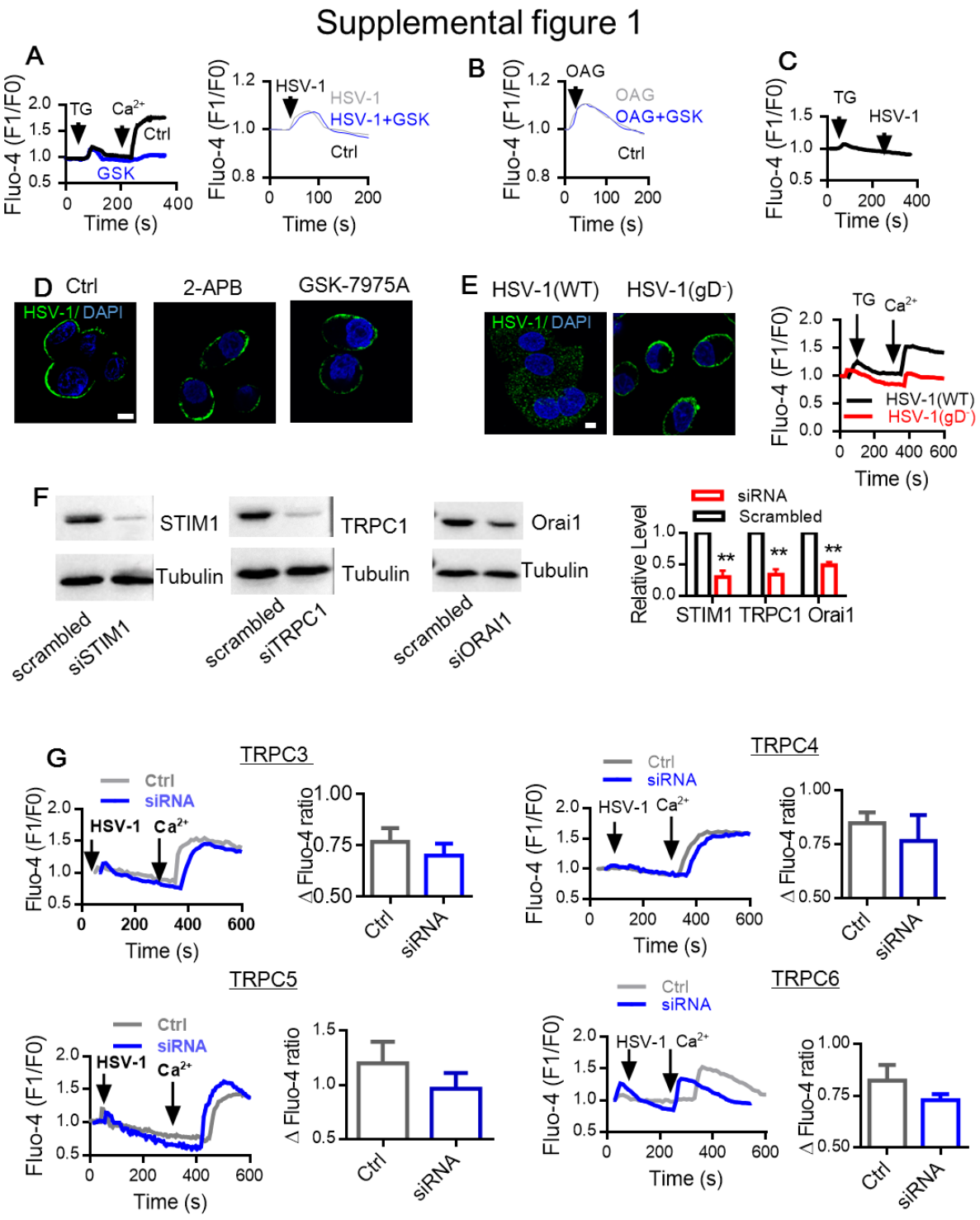

Fig. S1. Features of SOCE during HSV-1 infection. (**A**) GSK-7975A specifically inhibits SOCE. Left panel, Fluo-4-loaded HEp-2 cells were pretreated with 10 μM GSK-7975A for 10 min, or left untreated. Then TG was added (left arrow). After the Ca^{2+} efflux became stable, extracellular Ca^{2+} was added (right arrow). Right panel, Fluo-4/AM-loaded HEp-2 cells were pretreated with 10 μM GSK-7975A, or left untreated. Then infected with HSV-1 (arrow). For each condition, data were obtained from three replications, each of which included 10 cells,

meaning a total of 30 cells per condition [same for (B), (C), (E), and (G)]. (**B**) Effect of 1-oleoyl-2-acetyl-sn-glycerol (OAG)-induced Ca^{2+} influx. HEp-2 cells were pretreated with 10 μM GSK-7975A for 10 min, or left untreated. Then 100 μM OAG was added (arrow). (**C**) Effect of TG on HSV-1-induced Ca^{2+} influx. Fluo-4/AM-loaded HEp-2 cells were treated with TG (1^{st} arrow) before HSV-1 addition (2^{nd} arrow). (**D**) Inhibition of SOCE does not affect HSV-1 binding. Representative images of HEp-2 cells treated with 2-APB or GSK-7975A. HSV-1 binding was assessed by immunofluorescence (nuclei stained with DAPI; green, HSV-1). (**E**) Effect of gD-negative HSV-1 on HSV-1-induced Ca^{2+} influx. Left: gD-negative HSV-1 mutant fails to enter host cells as shown by immunofluorescence (nuclei stained with DAPI; green, HSV-1). Right, SOCE in gD-negative HSV-1-infected HEp-2 cells. SOCE was monitored as in (A). (**F**) Effect of siSTIM1, siOrai1, and siTRPC1 as analyzed by western blotting. Band intensities were normalized to that of loading control from the same gel. Then the results for siRNA groups were normalized to that of the scrambled siRNA and are shown as relative values (n = 3 blots for each treatment). (**G**) Effect of knockdown of TRPC channels in HSV-1-induced SOCE. TRPC3, C4, C5, and C6 siRNA were transfected into infected HEp-2 cells, and HSV-1-induced SOCE was monitored as in (A). $*P < 0.05$, $**P < 0.01$ by unpaired t-test (F and G); graphs show the mean ± SD; scale bars, 10 μm.

Supplemental figure 2

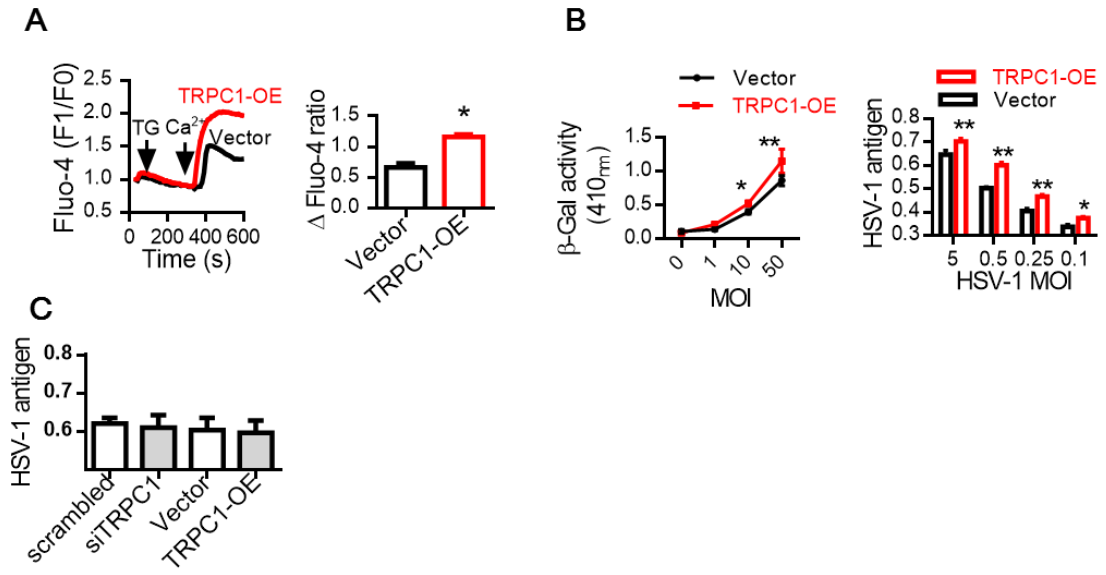

Fig. S2. TRPC1 modulates HSV-1 infection. (**A**) TRPC1 overexpression vector (TRPC1-OE) increases HSV-1-induced SOCE. TRPC1-OE-transfected HEp-2 cells were infected with 0.5 MOI of HSV-1 and then treated with TG (1st arrow). Ca^{2+} was added back to cells where indicated by 2nd arrow. Traces show relative fluorescence intensity. Bar graph to the right shows statistical analysis of peak fluorescence increase due to Ca^{2+} influx over the resting levels. For each condition, data were obtained from three replications, each of which included 10 cells, meaning a total of 30 cells per condition. (**B**) Effect of TRPC1-OE on HSV-1 infection. Entry (left) and replication (right) of HSV-1 analyzed with β-Gal assays and ELISA (n = 6 for each treatment). (**C**) siTRPC1 or TRPC1-OE does not affect HSV-1-binding as analyzed by ELISA (n = 6 for each treatment). **P* <0.05, ***P* <0.01 by unpaired t-test (A and C) and two-way ANOVA (B). Graphs show the mean ±SD.

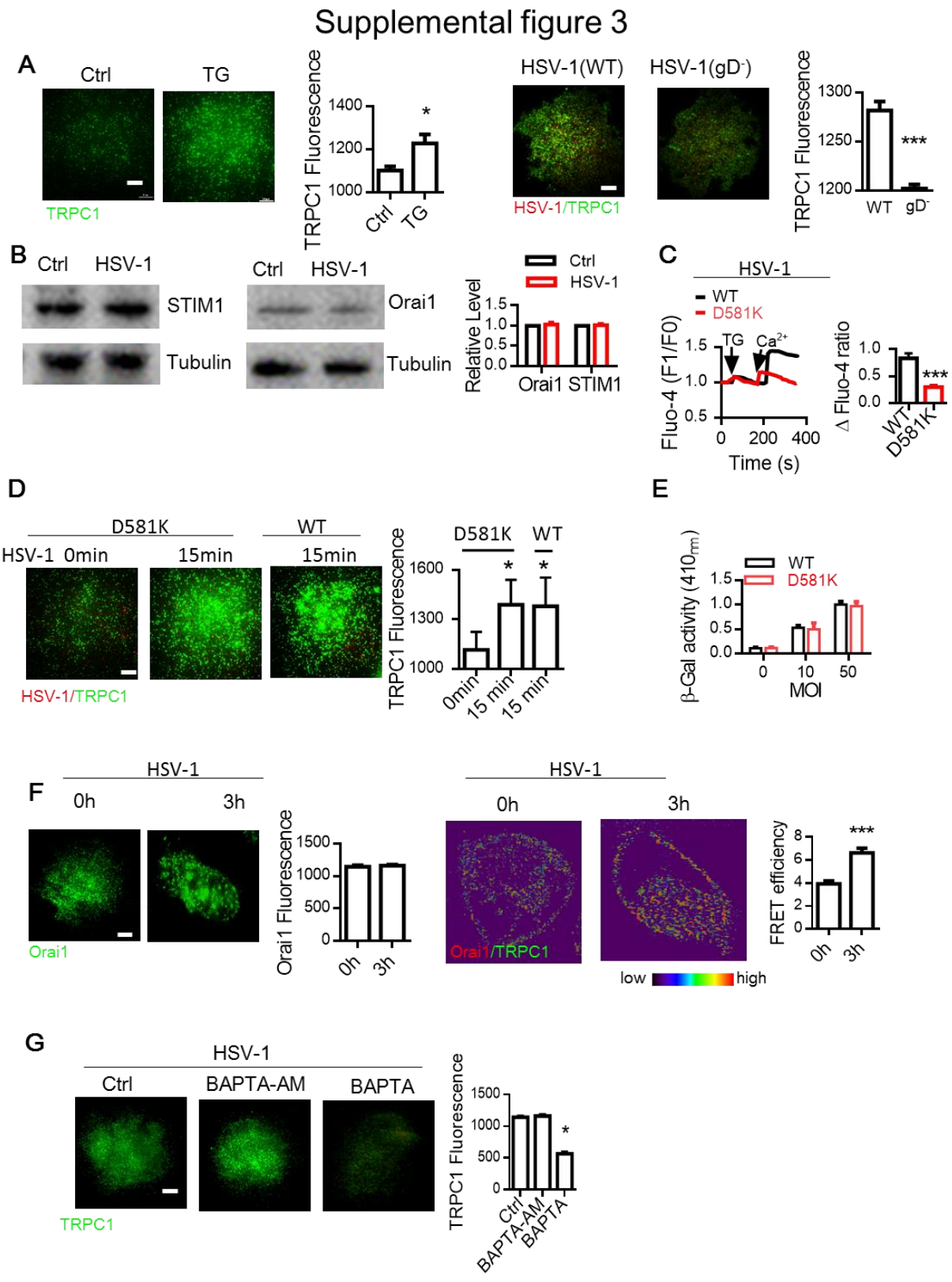

Fig. S3. Dynamic changes of SOCE-related molecules during HSV-1 infection. (**A**) Translocation of TRPC1 in HEp-2 cells. Representative TIRF microscope images of HEp-2 cells treated with 4 μM TG for 15 min (left) or infected with gD-negative HSV-1 (Right). For each condition, data were obtained from three replications, each of which included 5 cells,

meaning a total of 15 cells per condition, same in (C) (D) (F) and (G). (**B**) Effect of HSV-1 infection on Orai1 and STIM1 expression in HEp-2 cells. n = 3 blots for each treatment. Band intensities were normalized to that of loading control from the same gel. Then the results for HSV-1-infected group were normalized to that of the mock-infected control and are shown as relative values. (**C**) Effect of pore-dead mutant, $TRPC1^{D581K}$, on SOCE. WT TRPC1 and $TRPC1^{D581K}$-transfected HEp-2 cells were infected with 0.5 MOI of HSV-1 and then treated with TG (1^{st} arrow). Ca^{2+} was added back to cells where indicated by the 2^{nd} arrow. Traces show relative fluorescence intensity. Bar graph to the right shows statistical analysis of peak fluorescence increase due to Ca^{2+} influx over the resting levels. (**D**) $TRPC1^{D581K}$ does not impair TRPC1 translocation. HSV-1 was first allowed to bind to $TRPC1^{D581K}$- or WT TRPC1-transfected HEp-2 cells, then TRPC1 translocation was visualized after exposure to HSV-1 for 0 or 15 min by TIRF microscope. Scale bar, 10μm. (**E**) $TRPC1^{D581K}$ does not impair HSV-1 entry. HEp-2 cells were transfected with WT TRPC1 and $TRPC1^{D581K}$. Entry of HSV-1 was analyzed by β-Gal assay. (n = 6 for each treatment). (**F**) Effect of HSV-1 infection on Orai1 translocation. Left, representative images and statistics for Orai1 surface expression before (0 h) and after (3 h) HSV-1 entry analyzed by TIRF microscope; right, Orai1 and TRPC1 co-localization before (0 h) and after (3 h) HSV-1 entry analyzed by FRET. (**G**) Effects of BAPTA on TRPC1 translocation. HEp-2 cells were treated with 200 μM BAPTA-AM or BAPTA, then infected with HSV-1. TRPC1 translocation was analyzed by TIRF microscope. $*P < 0.05$, $***P < 0.001$ by unpaired t test (A, B, C and F), one-way ANOVA (D and G) and two-way ANOVA (E). Graphs show the mean ± SD. Scale bars, 10 μm.

Supplemental figure 4

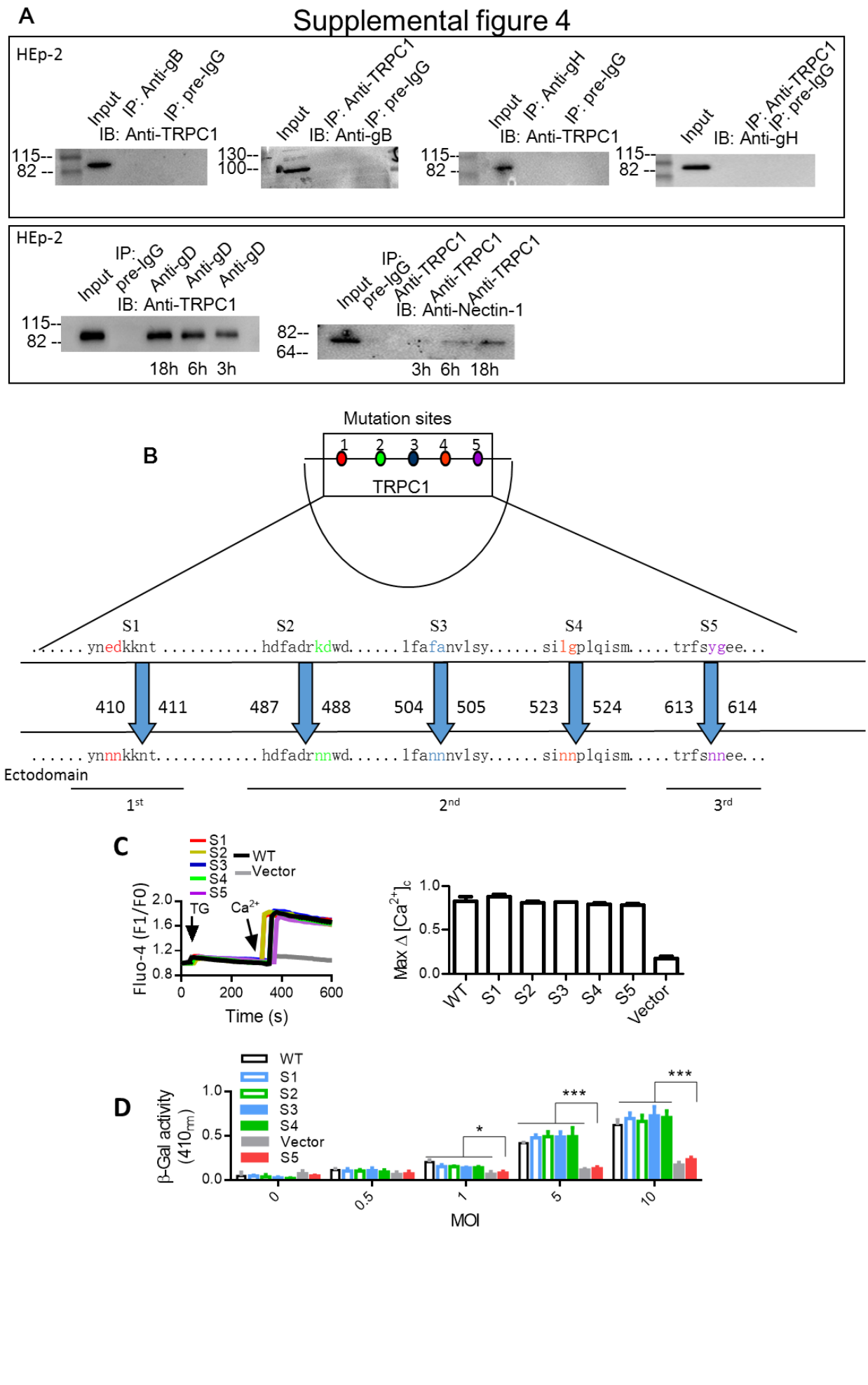

Fig. S4. Determination of gD-TRPC1 interaction. (**A**) Interactions between TRPC1 and HSV-1 glycoproteins. Upper panels, immunoprecipitation for gB or gH-TRPC1 interaction in HSV-1-infected HEp-2 cells; lower panels, after HSV-1 entered HEp-2 cells, gD was immunoprecipitated with TRPC1, and the presence of nectin-1 in the products of immunoprecipitation was analyzed by western blot. Pre-immune IgG served as a control. Input is the whole-cell extract as a positive control. (n = 3 blots for each treatment). (**B**) Mutation design of TRPC1. Five mutations (sites S1 to S5) were introduced into the ectodomains of human TRPC1 alpha (total length 793 AAs). The upper AA sequence is the original sequence in the ectodomains of TRPC1, and only part of the AA sequence around the mutation sites is shown. Site mutations were introduced, and their locations are shown next to the blue arrows. The mutated sequence is shown below. (**C**) Effect of TRPC1 mutants on SOCE. Five TRPC1 mutant (S1 to S5) were transfected into HEp-2 cells, and SOCE was analyzed as shown in fig. S2A. For each condition, data were obtained from three replications, each of which included 10 cells, meaning a total of 30 cells per condition. (**D**) Effect of TRPC1 mutants on HSV-1 entry into CHO cells. CHO cells were transfected with mutant TRPC1 (S1-S5) and then infected with HSV-1 gL86. Entry of HSV-1 was analyzed by β-Gal assays (n = 6 for each treatment). *P <0.05, ***P <0.001 by one-way ANOVA (C) and two-way ANOVA (D).

Supplemental figure 5

Fig. 2G

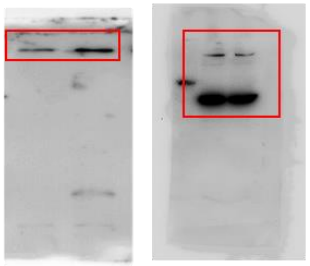

Fig. 3B

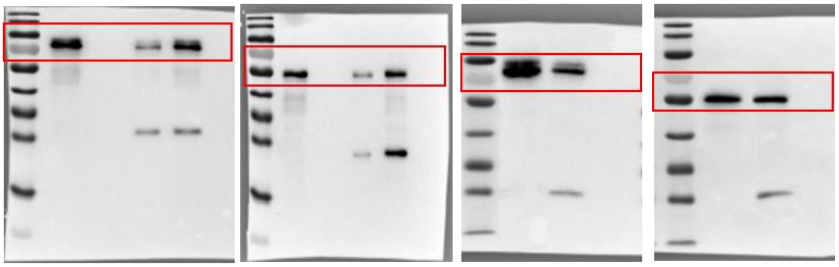

Fig. S1F

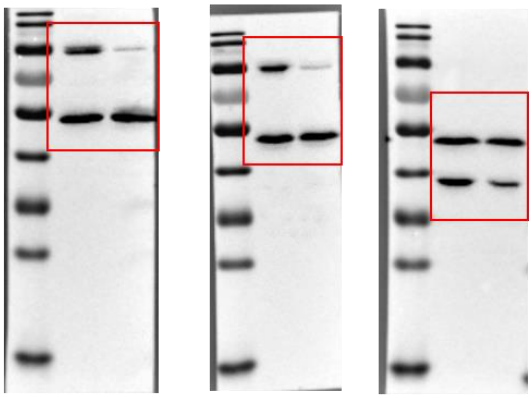

Fig. S3B

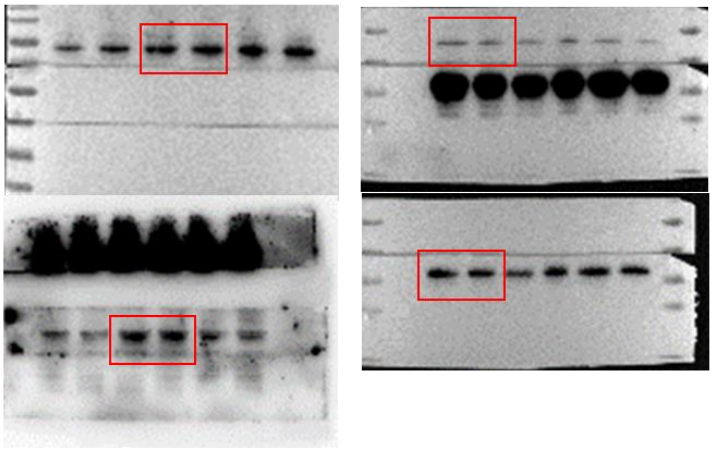

Fig. S4A

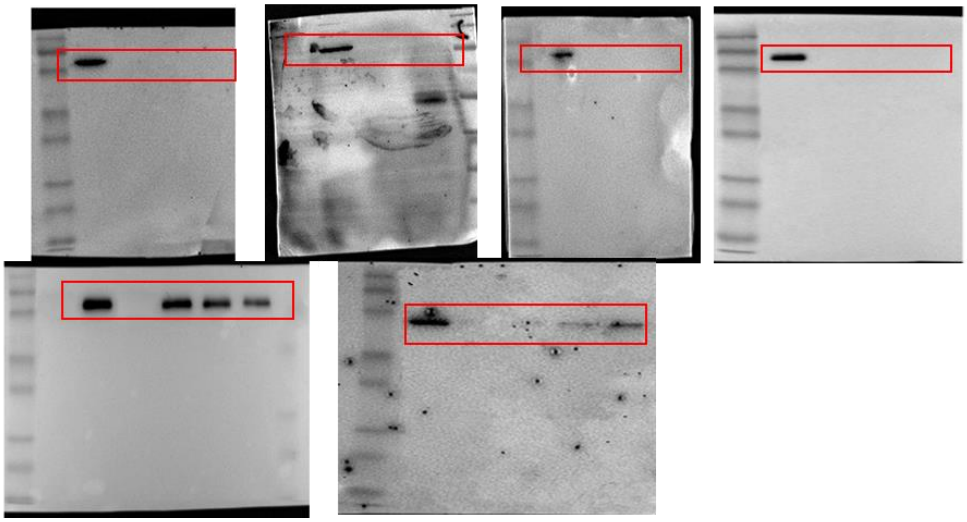

Fig. S5. Original images of Western blots.